

# Far-field Scatter Measurements of Planar Optical Waveguides using a Variable Launch System

Robert Ferguson, Irshaad Fatadin, Subrena Harris and James Allerton

*National Physical Laboratory, Teddington, Middlesex, TW11 0LW, U.K.*

Keywords: OPCB, Waveguides, Far-field.

Abstract: Polymer planar optical waveguides fabricated onto electrical printed circuit boards are an emerging technology to provide high-speed communications on computer backplanes. Along with the key parameters of attenuation and isolation, the variable launch system developed at NPL can now be used to measure the transmitted scatter profile of optical printed circuit boards (OPCBs) in order to explore the relationship between launch condition, waveguide and end-face quality. In this paper we describe the modifications to the existing NPL system and measurements of the far-field intensity profiles of a group of reference waveguides using a variety of spot sizes and numerical apertures.

## 1 INTRODUCTION

Polymer planar optical waveguides fabricated onto electrical printed circuit boards and incorporated onto computer backplanes are an emerging cost effective technology to facilitate high-speed data transfer in modern high speed computing and data storage systems. The integrated manufacture of these OPCBs has been investigated (Selviah, 2008, Bamiedakis, 2012) and is being further refined with demonstrators currently operating  $>10$  Gb/s. Their bandwidth capacity, size and lower energy demands ensure continuing interest among the leading international communications companies. Along with the technical demands of fabricating the boards or backplanes, a need to characterise the actual guides themselves is also essential. The optical performance of the waveguides is an important aspect to refining the manufacturing process (Kai Su, 2005). Currently these waveguides are multimoded, operating at 850 nm and intended for very high data rates. In addition to the fundamental parameters of attenuation and isolation, there is a need to understand the losses associated with the end-face surfaces and waveguide quality. An established system at NPL already measures the attenuation and isolation from the transmitted power and has the ability to vary the launch spot size and numerical aperture to fully explore the capability of these multi-mode waveguides (Ferguson, 2012). This system has now been modified to enable measurement scans of far-field intensity profiles across a range of different

launch conditions.

## 2 THE MODIFIED MEASUREMENT SYSTEM

The modified variable launch system is shown in Figure 1 and builds on previous work carried out at NPL (Ives, 2011, Ferguson, 2007). Light from an 850 nm VCSEL laser is launched into a step-index fibre with a  $365 \mu\text{m}$  core and a numerical aperture ( $NA$ ) of 0.22. The fibre is shaken at a few Hertz with an amplitude of a few millimetres to slowly scramble the speckle. The fibre provides the input illumination to the variable launch board. This allows the variation of the launch spot size, which is defined by a range of interchangeable pin-holes ranging from 5 to  $100 \mu\text{m}$  and the  $NA$  which is controlled by a variable aperture giving numerical apertures in the range 0.02 to 0.28. The launch board also includes a reference detector to monitor the launch power and a CCD with imaging optics to allow the alignment of the launch spot with the waveguide under test. The OPCB under test and the receive optics were mounted on movable stages. For attenuation measurements the output from the waveguide under test is imaged onto a CCD array to measure the total transmitted power. However, in order to measure the far-field intensity of the transmitted power  $P(\theta)$  a detector is scanned around an arc centred on the end of the waveguide under test. The

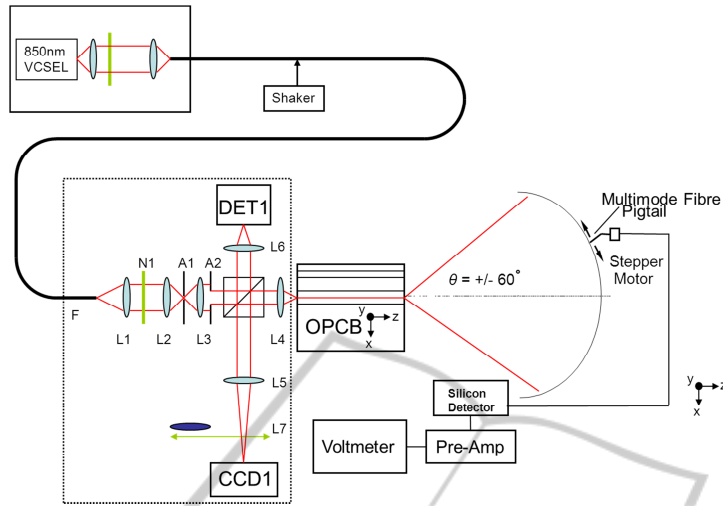


Figure 1: Measurement system optical layout. F = 365  $\mu\text{m}$  0.22 NA step index fibre; L1 = 50 mm focal length lens; L2, L3 and L4 = 16 mm focal length 0.4 NA objective; L5 = 150 mm focal length lens; L6 = 30 mm focal length lens; L7 = 60 mm focal length lens; N1 = neutral density filter; A1 = interchangeable pin-hole to set the launch spot size, A2 = variable aperture to control the launch spot NA. The CCD arrays image the near field surface of the waveguide, and with the addition of L7 can image the far field distribution.

detector comprises of a 100  $\mu\text{m}$  core diameter cleaved fibre pigtail mounted at the centre of a frustrum cone which is mounted on a rotation stage and scanned in angular steps of  $1^\circ$ . The fibre is connected to a silicon detector, pre-amplifier and voltmeter to measure the far-field intensity profiles. To ensure that the detector is in the far-field, the separation between the waveguide and the detector only needs to be greater than a few mm. However, to ensure good angular resolution the detector was located at 10 mm from the end of the waveguide. The size of the detector is another factor which determines the angular resolution, the fibre pigtail of a photodiode can provide a small area detector allowing the fibre-detector distance to be reduced without degrading the angular resolution. Reference measurements were made on the modified system using a characterised multimode fibre with an established value of  $0.195 \pm 0.005$  NA. The measured values ranged from 0.191 to  $0.208 \pm 0.01$  NA. The worst case Type A standard uncertainty (at  $\sim \pm 35^\circ$ ) is  $\pm 1.0$  dB. The uncertainties include the contributions associated with launch condition, the waveguide condition, the power measurements and the measurement repeatability and reproducibility. The uncertainties associated with the power measurement include the linearity of the reference detector. Uncertainties associated with the waveguide condition include the quality of the end faces and the alignment of the end face. All of these sources of uncertainty require further study.

### 3 END FACE QUALITY

To study the impact of surface roughness associated with the waveguides for the far-field measurements, a technique was developed to polish the end faces based on traditional optical glassworking methods. Surfaces were measured using a Taylor Hobson Form Taly-surf PGI 1000. The mean values as well as a typical surface scan are summarised below for the surface roughness measurements where  $R_v$  is the largest profile valley depth within the sampling length and  $R_a$  is the arithmetic mean of the absolute ordinate values within the sampling length (Leach, 2001). It can be seen that the polishing process significantly reduces the surface damage and produces surface qualities comparable to optically polished commercial optics. The resolution of the measuring instrument was  $\sim 12$  nm in the z-axis.

Wafer Sawn:	
End A: $R_v = 3.55 \mu\text{m} \pm 0.30 \mu\text{m}$ $R_a = 0.50 \mu\text{m} \pm 0.07 \mu\text{m}$	End B: $R_v = 2.83 \mu\text{m} \pm 0.46 \mu\text{m}$ $R_a = 0.33 \mu\text{m} \pm 0.10 \mu\text{m}$
Optically Polished:	
End A: $R_v = 0.20 \mu\text{m} \pm 0.05 \mu\text{m}$ $R_a = 0.06 \mu\text{m} \pm 0.03 \mu\text{m}$	End B: $R_v = 0.32 \mu\text{m} \pm 0.03 \mu\text{m}$ $R_a = 0.13 \mu\text{m} \pm 0.03 \mu\text{m}$

Figure 2: Scan length was  $\sim 3$  mm with 5 parallel runs carried out on each end of the board. Note that standard uncertainties are quoted.

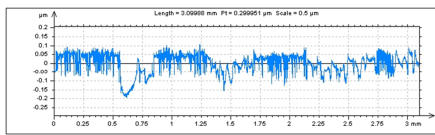


Figure 3: Typical surface roughness scan using the Talysurf PGI 1000 made on one of the polished ends of the sample.

#### 4 FAR-FIELD MEASUREMENTS OF TRANSMITTED POWER

Measurements were made on a sample group of 30 x 30 µm siloxane (Kai Su, 2005) waveguides, ~ 125 mm in length on an FR4 board produced using photolithography. The group was measured with both wafer sawn and polished end faces. Using the system described in Section 2, the transmitted power  $P(\theta)$  was measured over an angular scan range of  $\pm 60^\circ$  in  $1^\circ$  steps. At each angular measurement an average of 100 frames was taken to improve the signal-to-noise ratio and average the speckle. The entire measurement scan was repeated three times to monitor the stability of the launch. The measured power was normalised to the reference power and measured using the pick-off detector on the launch board, DET1. The camera CCD1 is only used to allow alignment and focussing of the launch spot onto the input surface of the waveguide under test. The launch NA was initially varied to investigate the subsequent changes in the scatter profile for the different surfaces using a spot size of 20 µm. More comprehensive measurements were then carried out on the sample waveguide group with the launch condition set to 0.16 NA and an under-filled spot of 20 µm in order to emulate typical integrated VCSEL sources. The NA was calculated using the sine of the half angle at which the far field intensity dropped to 5% of the peak value (IEC 60793-1-43 Ed. 1.0, 2001-07).

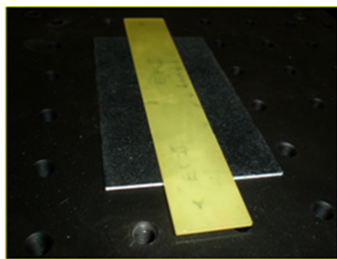


Figure 4: Sample OPCB containing groups of planar siloxane waveguides.

#### 5 LAUNCH NUMERICAL APERTURE COMPARISON

Changes were made to the launch condition by increasing the numerical aperture from between 0.02, 0.16 and 0.28 NA. Far-field scans were carried out with the end surfaces wafer sawn and with the ends optically polished. As expected, the profiles reveal a change in the exit NA with respect to the set launch condition NA as more modes are excited within the waveguide. However, the increase in the exit NA is minimal once the launch NA increases beyond 0.16 to 0.28. The greater scatter associated with wafer sawn surfaces shows a slight increase for each of the calculated NAs.

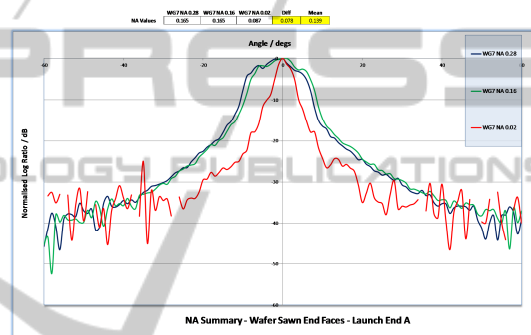


Figure 5: Far-field intensity scans of selected waveguides. The graph shows normalised signal against angle on sample with wafer sawn end faces with a launch at End A. Also shown are the calculated numerical apertures of each waveguide.

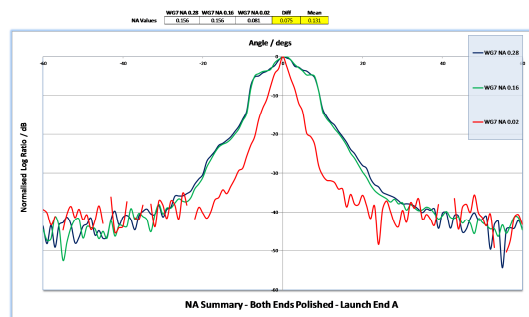


Figure 6: Far-field intensity scans of selected waveguides. The graph shows normalised signal against angle on sample with optically polished end faces with a launch at End A. Also shown are the calculated numerical apertures of each waveguide.

## 6 RESULTS AND UNCERTAINTIES

Figures 7 and 8 show the far-field scans for the selected group of waveguides with two different end-face surface treatments (with launches at ends designated A and B). For comparison measurements launched into end A are shown first. The greater scatter associated with the rougher surface of the wafer sawn end faces tends to obscure the asymmetry associated with the waveguides and their performance. The asymmetry of the scans is likely to be due to corresponding material asymmetries in the waveguide cross-section ie: a non-uniform refractive index profile across the waveguides and along their length. When looking at the waveguide group as launched from end B the plots compare well between the two different surface conditions. They also compare with the scan profiles when launched at end A, especially with the polished end faces. However, there is a clear difference for the waveguides number 5 and 6 where the scans exhibit a profile suggesting the presence of cladding modes. As the scan has not been mathematically corrected for any electrical field inversion they must be due to the presence of irregularities or defects affecting these particular waveguides.

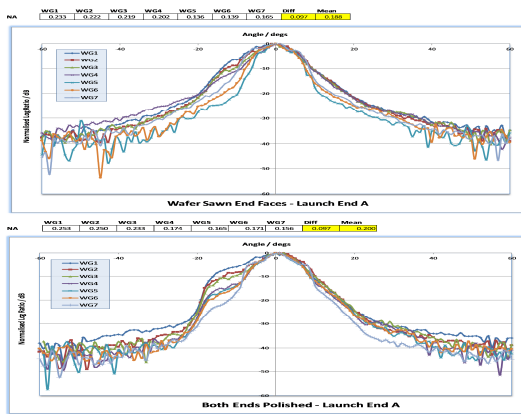


Figure 7: Far-field intensity scans of waveguide group containing 7 individual waveguides. Graph shows normalised signal against angle on sample with wafer sawn and polished end faces with a launch at End A. Also shown are the calculated numerical apertures of each waveguide.

## 7 FAR-FIELD DISCONTINUITIES

Further investigation of waveguides 5 and 6 showed how the far-field intensity profile can also be beneficial in revealing any manufacturing defects in the

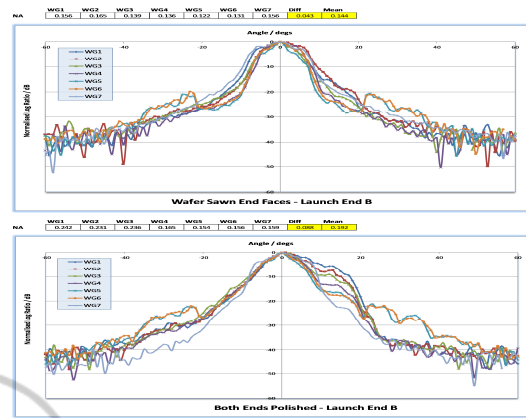


Figure 8: Far-field intensity scans of waveguide group containing 7 individual waveguides. Graph shows normalised signal against angle on sample with wafer sawn and polished end faces with a launch at End B. Also shown are the calculated numerical apertures of each waveguide.

waveguides. A defect was observed that lay between the two waveguide tracks, caused during the photolithographic manufacturing process. This produced subsequent discontinuities in the associated far-field scans (See Fig. 9)

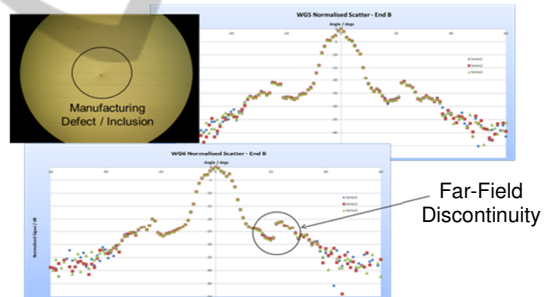


Figure 9: Far-field intensity scans of selected waveguides 5 and 6 affected by identifiable defect along waveguide length.

## 8 CONCLUSIONS

We have modified an existing system to investigate the far-field scatter of planar optical waveguides with respect to launch condition and end face quality. The scans have revealed that the dynamic range increases with polished faces (up to ~4 dB), which is consistent with the improvement in the total attenuation obtained through polishing the end faces. For each scan the exit numerical aperture of the waveguides with respect to the launch condition has been calculated from the far-field scan. Polishing has been shown to give

no advantage in terms of  $NA$  which only increases slightly when the board ends are polished from  $\sim 0.03$  to  $\sim 0.09 NA$ . An important feature of the work has been the ability to make use of the scanning process to detect board defects that can affect the performance of the waveguides. Discontinuities in the far-field profile relate to identifiable board defects or inclusions and the method has the potential to provide a rigorous technique to assess the quality of waveguide manufacture. Polishing appears to accentuate any waveguide inhomogeneity with the increased scatter due to the rougher wafer sawn surfaces masking any waveguide irregularities. There is evidence in the scans that suggests the waveguide performance is not always bi-directional. It is intended to use this set up to do a more systematic study of the transmission quality of waveguides produced using different methods and the relationship between launch conditions and the receive detectors deployed in working boards operating within data storage systems under a range of environmental conditions.

## ACKNOWLEDGEMENTS

We would like to thank Dr. Nikos Bamiedakis, Dr. Terry Clapp and Professor Richard Penty of Centre of Advanced Photonics and Electronics, Cambridge, for providing the sample waveguides and Neil Lockmuller of the Engineering Measurement Services Group at NPL for providing surface metrology support.

This work was supported by the Department for Business Innovation and Skills at NPL.

## REFERENCES

- D. R. Selviah, F. A. Fernandez, I. Papakonstantinou, K. Wang, H. Bagshiahi, A. C. Walker, A. McCarthy, H. Suyal, D. A. Hutt, P. P. Conway, J. Chappell, S. S. Zakariyah and D. Milward "Integrated optical and electronic interconnect printed circuit board manufacturing", *Circuit World*, vol. 34, pp. 21-26, 2008.
- Bamiedakis, N. Hashim, A., Penty, R. V., White, I. H., 'Regenerative polymeric bus architecture for board-level optical interconnects', *Optics Express* 11625, Vol 20, No. 11, 21 May 2012.
- Kai Su, Jon V. DeGroot, Jr., Ann W. Norris and Peter Y. Lo., 'Siloxane Materials for Optical Applications', *Advanced Technologies and Venture Business, Dow Corning Corporation*, 2200 W. Salzburg Road, Midland, MI, USA 48686. Proc. Of SPIE Vol. 6029 60291C-7, (2005).
- Ferguson, R., 'Waveguides Need Characterization, Too', *Photonics Spectra*, February 2012, pp.58-60.
- Ives, D., Ferguson, R. A., Harris, S., 'Development of a variable launch attenuation and isolation measurement system for optical waveguides', *Applied Optics*, Vol. 50, No. 22, 1 August 2011, pp. 4268 - 4275.
- R. A. Ferguson and S. Harris, "Development of an optical system with controlled launch conditions for the characterisation of polymer optical fibre (POF)", *Optical Fibre Measurement Conference Digest*, 15 October 2007.
- Leach, R. Measurement Good Practice Guide Number 37 - The Measurement of Surface Texture using Stylus Instruments, *National Physical Laboratory, Crown Copyright 2001*, ISSN 1368-6550, July 2001.
- IEC 60793-1-43 Optical fibres - Part 1-43: Measurement methods and test procedures - Numerical aperture, *Publication date 26-07-2001*.